Received: 6 September 2018 | Revised: 27 November 2018 | Accepted: 27 November 2018

DOI: 10.1002/rcm.8367

RESEARCH ARTICLE

WILEY Rapid Communications in Mass Spectrometry

Single-stranded DNA structural diversity: TAGGGT from monomers to dimers to tetramer formation

Jacob E. Porter[1] | Prem Chapagain[2,3] | Francisco Fernandez-Lima[1,3]

[1] Department of Chemistry & Biochemistry, Florida International University, Miami, FL, USA

[2] Department of Physics, Florida International University, Miami, FL, USA

[3] Biomolecular Sciences Institute, Florida International University, Miami, FL, USA

Correspondence
F. Fernandez-Lima, Department of Chemistry & Biochemistry, Florida International University, Miami, FL, USA.
Email: fernandf@fiu.edu

Funding information
National Science Foundation, Division of Chemistry, Grant/Award Number: CHE-1654274

Rationale: DNA quadruplex structures have emerged as novel drug targets due to their role in preventing abnormal gene transcription and maintaining telomere stability. Trapped Ion Mobility Spectrometry–Mass Spectrometry (TIMS–MS), combined with theoretical modeling, is a powerful tool for studying the kinetic intermediates of DNA complexes formed in solution and interrogated in the gas phase after desolvation.

Methods: A TAGGGT ssDNA sequence was purchased and studied in 10 mM ammonium acetate using nanospray electrospray ionization (nESI)-TIMS-MS in positive and negative ion mode. Collisional cross section (CCS) profiles were measured using internal calibration (Tune Mix). Theoretical structures were proposed based on molecular dynamics, charge location and geometry optimization for the most intense IMS bands based on the number of TAGGGT units, adduct form and charge states.

Results: A distribution of monomeric, dimeric and tetrameric TAGGGT structures were formed in solution and separated in the gas phase based on their mobility and *m/z* value (e.g., $[M+2H]^{+2}$, $[2M+3H]^{+3}$, $[M-2H]^{-2}$, $[2M-3H]^{-3}$, $[4M+4H]^{+4}$, $[4M+3H+NH_4]^{+4}$, $[4M+2H+2NH_4]^{+4}$ and $[4M+H+3NH_4]^{+4}$). The high mobility resolution of the TIMS-MS analyzer permitted the observation of multiple CCS bands per molecular ion form. Comparison with theoretical candidate structures suggests that monomeric TAGGGT species are stabilized by A-T and G^+-G interactions, with the size of the conformer influenced by the proton location. In the case of the TAGGGT quadruplex, the protonated species displayed a broad CCS distribution, while six discrete conformers were stabilized by the presence of ammonium ions ($n = 1–3$).

Conclusions: This is the first observation of multiple conformations of TAGGGT complexes ($n = 1$, 2 and 4) in 10 mM ammonium acetate. Candidate structures with intramolecular interactions of the form of G^+-G and traditional A-T base pairing agreed with the experimental trends. Our results demonstrate the structural diversity of TAGGGT monomers, dimers and tetramers in the gas phase beyond the previously reported solution structure, using 10 mM ammonium acetate to replicate biological conditions.

1 | INTRODUCTION

Beyond the classic double helical structures, DNA can exhibit a range of multi-stranded structures, including duplexes, triplexes, quadruplexes, cruciform structures and parallel-stranded structures.[1-5] In particular, quadruplexes have been the focus of recent research as drug targets, due to their role in protecting telomeric sequences from genetic instability,[6] as well as their presence in oncogene promoter regions.[7] While folding of telomeric DNA into G-quadruplexes has been hypothesized to protect against abnormal transcription,[8-11] more

recent research implies that they can drive genomic instability,[12,13] and they are overexpressed in certain cancer tissues.[14] Understanding the conditions and factors that stabilize these structures is an important part of many new cancer therapies.[15]

Multi-stranded topologies are traditionally identified and characterized using solution-phase techniques including NMR spectroscopy, X-ray diffraction, circular dichroism, calorimetry and IR spectroscopy.[16-19] However, many solution-phase techniques show only a single predominant solvent-stabilized structure or several closely related structures, and fail to characterize systems populated by multiple structures.[20] Complementary gas-phase studies using ion mobility spectrometry–mass spectrometry can provide insights into the structure of DNA complexes in the absence of solvent molecules. Results have shown that DNA complexes can be effectively trapped during the electrospray evaporative cooling into local minima that resemble the solution "native" conformations.[21,22] Several studies have been performed on transferring solution-phase quadruplex structures to the gas phase,[23,24] with structures usually stabilized in negative mode complexed to monovalent or trivalent ions.[25] Quadruplexes have shown particular affinity for K^+ and NH_4^+ in the gas phase,[26,27] with central ions necessary to prevent base mismatching and destabilization.[28,29]

In the present work, a custom model DNA sequence (TAGGGT) analogous to human telomeric sequences, known to adopt a four-stranded quadruplex structure in a solution,[30] was studied using Trapped Ion Mobility Spectrometry–Mass Spectrometry (TIMS-MS) and molecular dynamics. Candidate structures were suggested for the most abundant IMS bands and molecular ion forms. A discussion on the influence of the intra- and intermolecular base pairing on the TAGGGT structures is provided.

2 | EXPERIMENTAL

2.1 | Samples and reagents

Salt-free TAGGGT oligonucleotides were purchased (Eurofins Genomics) and used as received. The Tune Mix calibration standard was purchased from Agilent Inc. and used as received. All solvents and salts utilized in this study were analytical grade or higher. Samples were dissolved in 10 mM ammonium acetate (NH_4OAc) to a final concentration of 15–20 μM. Experiments were also carried out with solutions with various concentrations of KCl and NaCl, but no tetramer formation was observed. Annealing cycles (80°C) were performed prior to analysis, but no major effects were observed.

2.2 | TIMS-MS instrumentation and analysis

TIMS-MS provides complementary separations based on mobility (high resolving power, $R > 250–400$),[31,32] mass and charge, which allows the study of TAGGGT in the absence of the bulk solvent. TIMS operation and fundamentals have been described previously.[33-36] Briefly, ions are held stationary by a bath gas flow opposing an electric field, while radially confined using a quadrupolar radiofrequency (rf) field. An ion's reduced mobility, K_0, can be described by the following equation:

$$K_0 = \frac{V_g}{E_X} \approx A(1/(V_{out} - V_{elution}) \quad (1)$$

where v_g is the bath gas velocity, E_x is the electric field at which the ion elutes, V_{out} and $V_{elution}$ are the base and elution voltages, and K_0 is the reduced mobility. The calibration constant A was experimentally determined using compounds of known mobility (i.e., Tune Mix) as described elsewhere.[37] During TIMS operation, a number of ions are trapped simultaneously, based on the electric field range applied. Each ion may exist in multiple conformations, influenced by solvent and bath conditions and time after desolvation. After elution, ions are transferred to the mass spectrometer for mass analysis and detection. The total analysis time can be described by:

$$\begin{aligned}\text{Total IMS time} &= t_{trap} + (V_{elut}/V_{ramp})^* t_{ramp} + \text{ToF} \\ &= t_0 + (V_{elut}/V_{ramp})^* t_{ramp}\end{aligned}$$

where t_{trap} is the thermalization time, ToF is the time spent after the TIMS cell, and V_{ramp} and t_{ramp} are the voltage range and the scan time, respectively. t_0 in the simplified form of this equation refers to the time spent by ions outside the separation region (i.e. ion trapping and time-of-flight). t_0 and V_{elut} can be experimentally determined by varying the ramp time for a constant ramp voltage. Nitrogen was used as a bath gas at ca. 300 K, and the bath gas velocity was controlled by the pressure difference between the entrance funnel (P_1) and the exit funnel (P_2). P_1 and P_2 were kept constant at 2.5 mbar and 1.0 mbar, respectively. The TIMS cell was operated using a fill/trap/ramp/wait sequence of 14.5/.15/100–500/.765 ms. A constant 880 kHz 200 Vpp rf was applied to all electrodes including the entrance funnel, the TIMS analyzer section and the exit funnel (for schematic, see Figure S1, supporting information). Ions were introduced using low-energy conditions (i.e., $V_{Def} = \pm 60$ V, $V_{cap} = \pm 50$ V, and $V_{fun} = 0$ V) to avoid ion activation prior to the mobility analysis.[38,39] CCS (Ω) values were calculated from reduced mobility (K_0) values using the Mason-Schamp equation:

$$\Omega = \frac{18\pi^{1/2}}{16} \frac{z}{(K_B T)^{1/2}} \left[\frac{1}{m_I} + \frac{1}{m_b}\right]^{\frac{1}{2}} \frac{1}{K_0} \frac{1}{N^*}$$

where z is the charge of the ion, K_B is the Boltzmann constant, T is the temperature, N^* is the bath gas number density and m_I and m_b are the masses of the molecular ion and the bath gas, respectively.

2.3 | Theoretical modeling

Candidate structures were proposed based on a previously-outlined workflow.[40] Briefly, DNA models were adapted from the parallel-stranded quadruplex described by Patel et al (Protein Data Bank entry 1NP9).[30] Initial monomeric and dimeric structures were created by strand deletion, followed by molecular dynamics to replicate TIMS experimental conditions. Molecular dynamics simulations were performed in an NVT thermostat in YASARA software (www.yasara.org). The AMBER03 forcefield was used, which has proven validity for the study of nucleic acids.[41] The DNA was placed in a box extending 10 Å from each atom with periodic boundaries, which was populated with 10 N_2 molecules. A 10,000-step energy minimization was

performed using a conjugate gradient and line search algorithm, followed by an unconstrained simulation with a timestep of 2.5 fs. Snapshots were taken every 10,000 simulation steps, or every 25 ps, for a total of 4000 snapshots over a period of 100 ns. These 4000 structures were clustered into 40 groups using rmsd all vs. all calculations. Center of mass (CM) structures were chosen with the greatest similarity to the hypothetical centroid structure of each cluster, and the CCS value of each CM structure was calculated with the IMoS (version 1.04b)[42-44] package using nitrogen as a bath gas at *ca*. 300 K. A total of 100 rotations were performed using the trajectory method with a Maxwell distribution. These neutral structures were adapted with base-pair interactions taken from other Protein Data Bank entries; thymine:guanine interactions were taken from the dodecameric duplex d (CGCG AATTCGCG)$_2$, deposition 2BNA;[45] *cis*-guanine:guanine interactions were adapted from the eukaryotic TPP-specific riboswitch, deposition 3D2V, described by Thore et al;[46] finally, wobble thymine:guanine interactions were adapted from deposition 1VTT, a z-DNA d (CGCG TG) duplex described by Ho et al.[47] Four structures were constructed with interactions between A_2-T_6, T_1-G_5, T_1-G_4 and G_3-G_5, along with an additional structure with both A_2-T_6 and G_3-G_5 interactions. Each structure was then subjected to the previously described modeling process, with each nitrogenous base-pair constrained and a shorter timestep (4 fs, with a snapshot taken each 6250 steps). Protonated candidates were constructed based on previous computational studies of protonated base-pair interactions, including G-G, A-G, T-G and A-T.[48-50] The same procedure was used to model the dimeric species, with monomeric species adapted to include intramolecular G_3-G_5 interactions and intermolecular T_1-A_2 interactions, followed by constrained modeling. Other species were also considered, including a duplex with each base interacting, a duplex with strand slippage, and unconstrained molecular modeling.

3 | RESULTS AND DISCUSSION

Figure 1 shows typical mobility profiles of the monomer of TAGGGT in positive and negative ion mode, with MS projections in the inset. Inspection of Figure 1 shows a single broad band (C) for the $[M - 2H]^{-2}$ molecular ion, while multiple bands are observed for the $[M + 2H]^{+2}$ and $[M + H + Na]^{+2}$ molecular ions. Previous research on DNA-drug complexes in negative mode suggests that, in spite of the differences in ionization between positive and negative mode, many of the same structures and hydrogen-bonding interactions are retained.[51] In negative mode, several phosphates are protonated by interactions with ammonium ions, leaving the rest deprotonated.[52] The better-defined IMS bands observed in positive mode suggest that nucleobase protonation restricts the number of potential conformers via stabilization of non-canonical base-pairing, in good agreement with previous theoretical studies.[53,54] This is in contrast to certain broader bands in positive mode (i.e. bands D and L) which are indicative of less tightly folded conformers, similar to those previously observed in nESI-TIMS experiments on DNA structures.[21] Sodium adduction has been shown to stabilize both larger and smaller structures in gas-phase analysis of small molecules and peptides.[55-57]

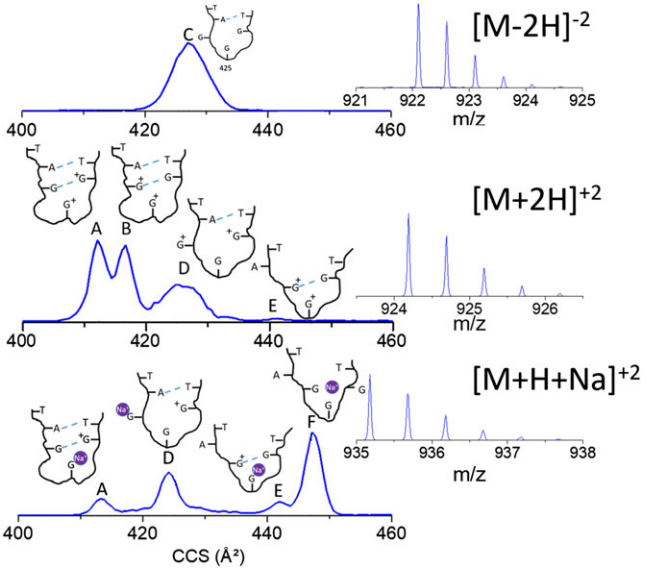

FIGURE 1 Typical IMS profiles of TAGGGT showing $[M - 2H]^{-2}$ (top), $[M + 2H]^{+2}$ (middle) and $[M + H + Na]^{+2}$ (bottom) and corresponding MS projections (see inset). Schematics highlighting the main features of the candidate structures proposed for each band are shown [Color figure can be viewed at wileyonlinelibrary.com]

Comparison between the $[M + 2H]^{+2}$ and $[M + H + Na]^{+2}$ profiles showed some common bands, which can be assigned to similar conformational motifs (A, B, D, and E), while a high CCS band (F) predominated for the $[M + H + Na]^{+2}$ molecular ion. A summary is provided in Table S1 (supporting information).

Candidate structures were proposed for all the mobility bands and molecular ion forms contained in Figure 1. The candidate structures proposed for bands A and B share A_2-T_6 and G_3-G_5 interactions; both are protonated on the N_7 atom of G_4, and contain a G:G W:H Cis interaction, as described by Halder et al.[48] The A and B candidate structures differ by protonation of the G_3-G_5 pair. Protonation on the N_7 atom of G_5 corresponds to structure A, as it is several Å^2 smaller than the candidate proposed for B with protonation on the N_7 atom of G_3. The candidate structure proposed for band D retains the A_2-T_6 interaction and loses the G_4-G_6 interaction, with protonation on the N_7 atoms of both G_4 and G_6. The candidate structure proposed for band E is protonated on the N_7 atoms of both G_3 and G_4, and loses the the A_2-T_6 interaction. A larger structure corresponding to conformer F shares no intramolecular interactions due to the sodium cation; the disruption of intramolecular interactions between bases in the presence of sodium has been previously observed.[58]

Figure 2 shows typical IMS profiles of the dimer of TAGGGT in negative and positive ion mode. Six distinct and two broad mobility bands are observed in positive and negative ion mode, respectively.

Inspection of the candidate structures shows stabilization via canonical base pairing ($1T_1$-$2A_2$ and $1A_2$-$2T_1$) for the most abundant IMS bands in positive mode (H, J, and K). These CCS values overlap with the broad band I in negative mode. This supports the idea that A-T interactions are preserved in negative ion mode, with additional interactions locking the structure into specific conformers in positive ion mode. For example, candidate structures for bands J and K have

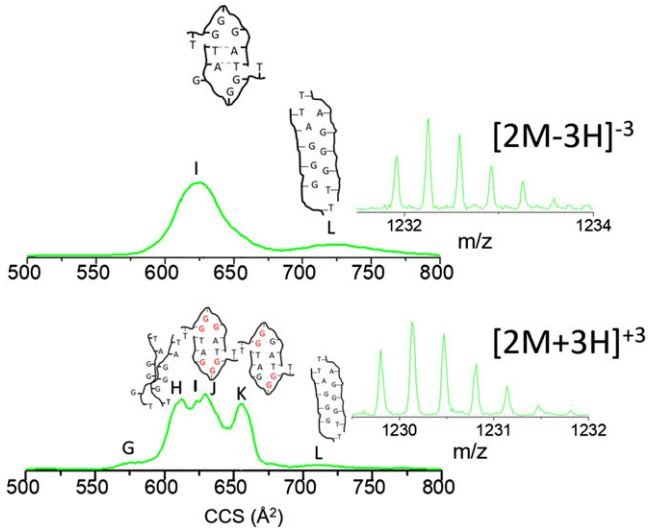

FIGURE 2 Typical IMS profiles of $[2M - 3H]^{-3}$ (top) and $[2M + 3H]^{+3}$ (bottom) and corresponding MS projections (see inset). Schematics highlighting the main features of the candidate structures proposed for each band are shown [Color figure can be viewed at wileyonlinelibrary.com]

additional stabilization via the G_3-G_5 intramolecular interaction, while a structure corresponding to band H was obtained by fixing the $1A_2$-$2T_1$ and $1T_1$-$2A_2$ interactions and unpairing the remaining bases. Candidate structures corresponding to band L, which is present in both positive and negative mode, were obtained by unpairing of all bases. Structures obtained by parallel-stranded interaction and base slippage resulted in much larger CCS values than band L. 2D Schematics corresponding to monomeric and dimeric theoretical structures can be seen in Figure S2 (supporting information).

Figure 3 shows the mobility profiles and mass spectrum of the tetrameric species in positive mode. A very broad mobility distribution (~450 Å^2 across) is observed for the protonated species $[4M + 4H]^{+4}$; however, in the presence of ammonium adducts (n = 1–3), six distinct IMS bands are observed (bands M–R). In the case of the TAGGGT tetramer, we did not observe a molecular ion in negative ion mode; previous studies with other quadruplexes have been carried out exclusively in negative ion mode.[29,59,60] A rigid intermolecular quadruplex formed from TGGGGT strands has been previously observed at a CCS value of 1010 Å^2, which correlates well with band M in our experiment.[60] Prior studies were carried out in solutions with 50–200 mM ammonium acetate;[61] the lower concentration of ammonium acetate (10 mM) may explain the broad CCS space where species outside of band M may come from mismatching/destabilization. Association rate constants for this particular sequence are also relatively low, as there are only three guanines in the central G-tract and two destabilizing thymines.[62] These factors imply that the tetrameric conformational space may not entirely represent a solution-phase quadruplex.

The wide IMS profiles observed for the tetrameric species are consistent with previous results of i-motif DNA;[22] the presence of inner cations may also induce preference for alternative kinetically trapped conformations in the gas phase. For example, closer inspection of the +4 charge state distributions showed the presence

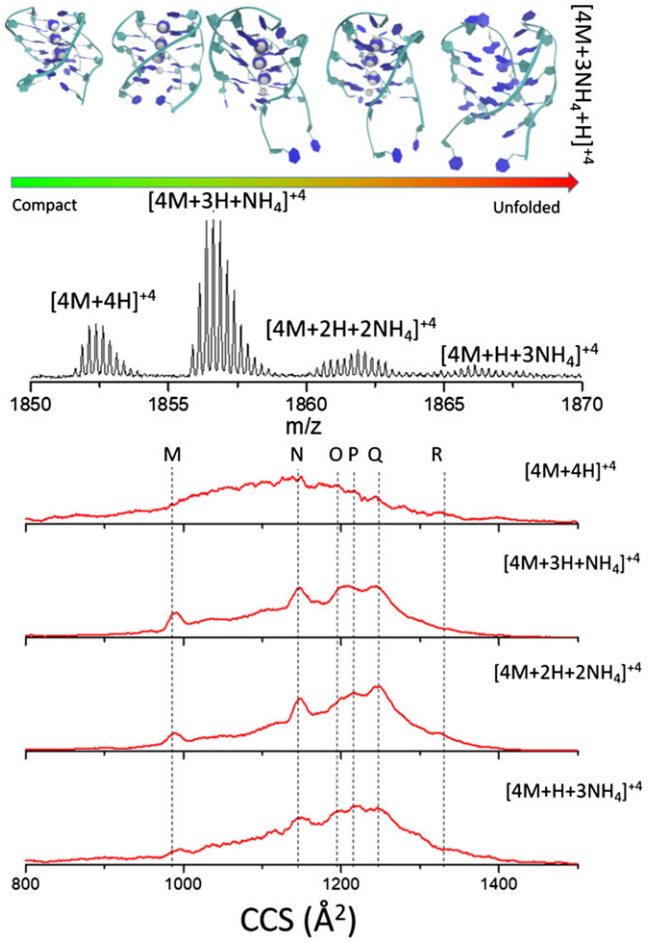

FIGURE 3 Typical MS (middle) and IMS projections (bottom) of the $[4M + 4H]^{+4}$, $[4M + 3H + NH4]^{+4}$, $[4M + 2H + 2NH4]^{+4}$ and $[4M + H + 3NH4]^{+4}$ species (bottom) and candidate structures (from smallest to largest). Schematics highlighting the main features of the candidate structures proposed for each band are shown [Color figure can be viewed at wileyonlinelibrary.com]

of ammonium adducts. These adducts can be attached to the structure and result in: (i) no conformational changes (no shift in the IMS profile), or (ii) can stabilize the structure in other folding states (changes in relative abundance and better-resolved bands in the IMS profile).

Inspection of the proposed candidate structures M–R suggest a proton located between the third G-tetrad and the adenines. The adenines lack oxygens, and so cannot hydrogen bond to an ammonium ion. The presence of a proton instead decreases the stability of the quadruplex, allowing for the bases to unfold and form larger structures. The IMS band N corresponds to the reported solution structure for the TAGGGT quadruplex.[30] A smaller conformer, M, can be obtained by a reduction along the z-axis (~75%) of the solution structure (band N) that may be explained by a gas-phase collapse. Candidate structures proposed for bands O–Q show unfolding of the T1 and A2 bases, while the candidate structures obtained for band R show the loss of intermolecular interactions between the DNA bases. Theoretical structures proposed for monomeric, dimeric and tetrameric species along with corresponding CCS values are presented in Figure S3 (supporting information).

While proposed structures for monomeric, dimeric and tetrameric species show good agreement with the CCS values of the observed mobility bands, they should be considered as suggestions rather than conclusive assignments due to several factors. Structures are not fully converged since the force field parameters are optimized for solution-phase samples with implicit solvent molecules. In addition, initial candidate structures were created with base-pair interactions taken into consideration; while additional hydrogen-bonding interactions between phosphates and sugars were observed during trajectory method modeling, these were not explicitly considered or used for proposing candidate structures. As such, the theoretical structural space explored in this paper is not comprehensive.

4 | CONCLUSIONS

Multiple mobility bands were observed for the TAGGGT as a function of the oligomerization state (n = 1,2 and 4) and molecular ion form (i.e., deprotonated, protonated and with sodium and ammonium adducts). The comparison with candidate structures suggested that stabilization can be due to intra- and intermolecular interaction via canonical (A-T) and non-canonical (G^+-G) base pairing. The gas-phase studies allowed for the observation of multiple TAGGGT tetramers, including the previously reported solution quadruplex structure.[30] This study reveals the structural diversity of ssDNA and the influence of the charge sites on the stabilization of the tridimensional structure. Development of more accurate force fields, in the absence of the solvent, will significantly improve the comparison of candidate structures with TIMS-MS results.

ACKNOWLEDGEMENTS

This work was supported by the National Science Foundation, Division of Chemistry (under CAREER award CHE-1654274) with co-funding from the Division of Molecular and Cellular Biosciences to F.F.-L.

ORCID

Francisco Fernandez-Lima https://orcid.org/0000-0002-1283-4390

REFERENCES

1. Limongelli V, De Tito S, Cerofolini L, et al. The G-triplex DNA. *Angew Chem Int Ed*. 2013;52(8):2269-2273.
2. Parvathy VR, Bhaumik SR, Chary KVR, et al. NMR structure of a parallel-stranded DNA duplex at atomic resolution. *Nucleic Acids Res*. 2002;30(7):1500-1511.
3. Plum GE, Park YW, Singleton SF, Dervan PB, Breslauer KJ. Thermodynamic characterization of the stability and the melting behavior of a DNA triplex: A spectroscopic and calorimetric study. *Proc Natl Acad Sci*. 1990;87(23):9436-9440.
4. Shchyolkina AK, Borisova OF, Livshits MA, Jovin TM. Parallel-stranded DNA with natural base sequences. *J Mol Biol*. 2003;37(2):223-231.
5. Kaushik M, Kaushik S, Roy K, et al. A bouquet of DNA structures: Emerging diversity. *Biochem Biophys Rep*. 2016;5:388-395.
6. Moye AL, Porter KC, Cohen SB, et al. Telomeric G-quadruplexes are a substrate and site of localization for human telomerase. *Nat Commun*. 2015;6(1):7643.
7. Yuan L, Tian T, Chen Y, et al. Existence of G-quadruplex structures in promoter region of oncogenes confirmed by G-quadruplex DNA cross-linking strategy. *Sci Rep*. 2013;3(1):1811.
8. Sissi C, Lucatello L, Cadamuro SA, Zagotto G, Palumbo M, Fox K. G-quadruplex stabilization by anthraquinone-peptide conjugates. *J Cancer Res*. 2006;66(8 Supplement):1172.
9. Mergny J-L, Hélène C. G-quadruplex DNA: A target for drug design. *Nat Med*. 1998;4(12):1366-1367.
10. Balasubramanian S, Hurley LH, Neidle S. Targeting G-quadruplexes in gene promoters: A novel anticancer strategy? *Nat Rev Drug Discov*. 2011;10(4):261-275.
11. Huang F-C, Chang C-C, Wang J-M, Chang T-C, Lin J-J. Induction of senescence in cancer cells by the G-quadruplex stabilizer, BMVC4, is independent of its telomerase inhibitory activity. *Br J Pharmacol*. 2012;167(2):393-406.
12. Wang Y, Yang J, Wu WH, et al. G-quadruplex DNA drives genomic instability and represents a targetable molecular abnormality in ATRX-deficient malignant glioma. *bioRxiv*. 2018.
13. Zybailov BL, Sherpa MD, Glazko GV, Raney KD, Glazko VI. G4-quadruplexes and genome instability. *J Mol Biol*. 2013;47(2):197-204.
14. Biffi G, Tannahill D, Miller J, Howat WJ, Balasubramanian S. Elevated levels of G-Quadruplex formation in human stomach and liver Cancer tissues. *PLoS ONE*. 2014;9(7):e102711.
15. Yang D, Okamoto K. Structural insights into G-quadruplexes: Towards new anticancer drugs. *Future Med Chem*. 2010;2(4):619-646.
16. Tereshko V, Wilds CJ, Minasov G, et al. Detection of alkali metal ions in DNA crystals using state-of-the-art x-ray diffraction experiments. *Nucleic Acids Res*. 2001;29(5):1208-1215.
17. Smith FW, Feigon J. Quadruplex structure of Oxytricha telomeric DNA oligonucleotides. *Nature*. 1992;356(6365):164-168.
18. Andrushchenko V, Tsankov D, Krasteva M, Wieser H, Bour P. Spectroscopic detection of DNA quadruplexes by vibrational circular dichroism. *J Am Chem Soc*. 2011;133(38):15055-15064.
19. Duguid JG, Bloomfield VA, Benevides JM, Thomas GJ Jr. DNA melting investigated by differential scanning calorimetry and Raman spectroscopy. *Biophys J*. 1996;71(6):3350-3360.
20. Wang Y, Patel DJ. Solution structure of a parallel-stranded G-Quadruplex DNA. *J Mol Biol*. 1993;234(4):1171-1183.
21. Garabedian A, Baird MA, Porter J, et al. Linear and differential ion mobility separations of middle-down Proteoforms. *Anal Chem*. 2018;90(4):2918-2925.
22. Arcella A, Portella G, Orozco M. Structure of Nucleic Acids in the Gas Phase. In: Gabelica V, ed. *Nucleic Acids in the Gas Phase*. Berlin, Heidelberg: Springer Berlin Heidelberg; 2014:55-75.
23. Scalabrin M, Palumbo M, Richter SN. Highly improved electrospray ionization-mass spectrometry detection of G-Quadruplex-folded oligonucleotides and their complexes with small molecules. *Anal Chem*. 2017;89(17):8632-8637.
24. Marchand A, Gabelica V. Folding and misfolding pathways of G-quadruplex DNA. *Nucleic Acids Res*. 2016;44(22):10999-11012.
25. Bhattacharyya D, Mirihana Arachchilage G, Basu S. Metal Cations in G-Quadruplex Folding and Stability. *Front Chem*. 2016;4:38.
26. Schultze P, Hud NV, Smith FW, Feigon J. The effect of sodium, potassium and ammonium ions on the conformation of the dimeric quadruplex formed by the Oxytricha nova telomere repeat oligonucleotide d(G(4)T(4)G(4)). *Nucleic Acids Res*. 1999;27(15):3018-3028.
27. Marchand A, Gabelica V. Native electrospray mass spectrometry of DNA G-Quadruplexes in potassium solution. *J Am Soc Mass Spectrom*. 2014;25(7):1146-1154.
28. Wang Z, Liu J-P. Effects of the central potassium ions on the G-quadruplex and stabilizer binding. *J Mol Graph Model*. 2017;72:168-177.

29. Balthasart F, Plavec J, Gabelica V. Ammonium ion binding to DNA G-quadruplexes: Do electrospray mass spectra faithfully reflect the solution-phase species? *J Am Soc Mass Spectrom*. 2013;24(1):1-8.
30. Patel PK, Koti AS, Hosur RV. NMR studies on truncated sequences of human telomeric DNA: Observation of a novel A-tetrad. *Nucleic Acids Res*. 1999;27(19):3836-3843.
31. Adams KJ, Montero D, Aga D, Fernandez-Lima F. Isomer separation of polybrominated diphenyl ether metabolites using nanoESI-TIMS-MS. *Int J Ion Mobil Spectrom*. 2016;19(2):69-76.
32. Silveira JA, Ridgeway ME, Park MA. High resolution trapped ion mobility Spectrometery of peptides. *Anal Chem*. 2014;86(12):5624-5627.
33. Fernandez-Lima F, Kaplan DA, Suetering J, Park MA. Gas-phase separation using a trapped ion mobility spectrometer. *Int J Ion Mobil Spectrom*. 2011;14(2–3):93-98.
34. Fernandez-Lima FA, Kaplan DA, Park MA. Note: Integration of trapped ion mobility spectrometry with mass spectrometry. *Rev Sci Instrum*. 2011;82(12):126106.
35. Silveira JA, Michelmann K, Ridgeway ME, Park MA. Fundamentals of trapped ion mobility spectrometry part II: Fluid dynamics. *J Am Soc Mass Spectrom*. 2016;27(4):585-595.
36. Michelmann K, Silveira JA, Ridgeway ME, Park MA. Fundamentals of trapped ion mobility spectrometry. *J Am Soc Mass Spectrom*. 2015;26(1):14-24.
37. Hernandez DR, DeBord JD, Ridgeway ME, Kaplan DA, Park MA, Fernandez-Lima F. Ion dynamics in a trapped ion mobility spectrometer. *Analyst*. 2014;139(8):1913-1921.
38. Molano-Arevalo JC, Hernandez DR, Gonzalez WG, et al. Flavin adenine dinucleotide structural motifs: From solution to gas phase. *Anal Chem*. 2014;86(20):10223-10230.
39. Molano-Arevalo JC, Gonzalez W, Jeanne Dit Fouque K, Miksovska J, Maitre P, Fernandez-Lima F. Insights from ion mobility-mass spectrometry, infrared spectroscopy, and molecular dynamics simulations on nicotinamide adenine dinucleotide structural dynamics: NAD+vs. NADH. *PCCP*. 2018;20(10):7043-7052.
40. Schenk ER, Nau F, Fernandez-Lima F. Theoretical predictor for candidate structure assignment from IMS data of biomolecule-related conformational space. *Int J Ion Mobil Spectrom*. 2015;18(1):23-29.
41. Ricci CG, de Andrade ASC, Mottin M, Netz PA. Molecular dynamics of DNA: Comparison of force fields and terminal nucleotide definitions. *J Phys Chem B*. 2010;114(30):9882-9893.
42. Larriba C, Hogan CJ Jr. Ion Mobilities in diatomic gases: Measurement versus prediction with non-specular scattering models. *J Phys Chem a*. 2013;117(19):3887-3901.
43. Larriba C, Hogan CJ Jr. Free molecular collision cross section calculation methods for nanoparticles and complex ions with energy accommodation. *J Comput Phys*. 2013;251:344-363.
44. Ouyang H, Larriba-Andaluz C, Oberreit DR, Hogan CJ Jr. The collision cross sections of iodide salt cluster ions in air via differential mobility analysis-mass spectrometry. *J Am Soc Mass Spectrom*. 2013;24(12):1833-1847.
45. Holbrook SR, Dickerson RE, Kim S-H. Anisotropic thermal-parameter refinement of the DNA dodecamer CGCGAATTCGCG by the segmented rigid-body method. *Acta Cryst B*. 1985;41(4):255-262.
46. Thore S, Frick C, Ban N. Structural basis of thiamine pyrophosphate analogues binding to the eukaryotic riboswitch. *J Am Chem Soc*. 2008;130(26):8116-8117.
47. Ho PS, Frederick CA, Quigley GJ, et al. G. T wobble base-pairing in Z-DNA at 1.0 a atomic resolution: The crystal structure of d (CGCG TG). *EMBO J*. 1985;4(13A):3617-3623.
48. Halder A, Bhattacharya S, Datta A, Bhattacharyya D, Mitra A. The role of N7 protonation of guanine in determining the structure, stability and function of RNA base pairs. *Phys Chem Chem Phys*. 2015;17(39):26249-26263.
49. Noguera M, Sodupe M, Bertrán J. Effects of protonation on proton transfer processes in Watson–crick adenine–thymine base pair. *Theor Chem Acc*. 2007;118(1):113-121.
50. Sun L, Bu Y, Qiao Q, Liu Q, Guo Z. The effect of ionization and deprotonation of guanine on the formation of base pairs. *Comput Theor Chem*. 2012;980(Supplement C):23-31.
51. Rosu F, Pirotte S, Pauw ED, Gabelica V. Positive and negative ion mode ESI-MS and MS/MS for studying drug–DNA complexes. *Int J Mass Spectrom*. 2006;253(3):156-171.
52. Green-Church KB, Limbach PA. Mononucleotide gas-phase proton affinities as determined by the kinetic method. *J Am Soc Mass Spectrom*. 2000;11(1):24-32.
53. Halder A, Halder S, Bhattacharyya D, Mitra A. Feasibility of occurrence of different types of protonated base pairs in RNA: A quantum chemical study. *PCCP*. 2014;16(34):18383-18396.
54. Jissy AK, Datta A. Designing molecular switches based on DNA-base mispairing. *J Phys Chem B*. 2010;114(46):15311-15318.
55. Zietek BM, Mengerink Y, Jordens J, Somsen GW, Kool J, Honing M. Adduct-ion formation in trapped ion mobility spectrometry as a potential tool for studying molecular structures and conformations. *Int J Ion Mobil Spectrom*. 2017;21(1-2):19-32.
56. Seo Y, Schenauer MR, Leary JA. Biologically relevant metal-cation binding induces conformational changes in heparin oligosaccharides as measured by ion mobility mass spectrometry. *Int J Mass Spectrom*. 2011;303(2–3):191-198.
57. Wu C, Klasmeier J, Hill HH. Atmospheric pressure ion mobility spectrometry of protonated and sodiated peptides. *Rapid Commun Mass Spectrom*. 1999;13(12):1138-1142.
58. Chaires JB. Human telomeric G-quadruplex: Thermodynamic and kinetic studies of telomeric quadruplex stability. *FEBS J*. 2010;277(5):1098-1106.
59. Gidden J, Baker ES, Ferzoco A, Bowers MT. Structural motifs of DNA complexes in the gas phase. *Int J Mass Spectrom*. 2005;240(3):183-193.
60. D'Atri V, Porrini M, Rosu F, Gabelica V. Linking molecular models with ion mobility experiments. Illustration with a rigid nucleic acid structure. *J Mass Spectrom*. 2015;50(5):711-726.
61. Kolesnikova S, Hubálek M, Bednárová L, Cvacka J, Curtis EA. Multimerization rules for G-quadruplexes. *Nucleic Acids Res*. 2017;45(15):8684-8696.
62. Neidle S, Balasubramanian S. *Energetics, Kinetics and Dynamics of Quadruplex Folding*. Quadruplex Nucleic Acids: The Royal Society of Chemistry; 2006:31-80.

SUPPORTING INFORMATION

Additional supporting information may be found online in the Supporting Information section at the end of the article.

How to cite this article: Porter JE, Chapagain P, Fernandez-Lima F. Single-stranded DNA structural diversity: TAGGGT from monomers to dimers to tetramer formation. *Rapid Commun Mass Spectrom*. 2019;1-6. https://doi.org/10.1002/rcm.8367